

Aggregation Model Hyperparameters Matter in Digital Pathology

Gustav Bredell, Marcel Fischer, Przemyslaw Szostak, Samaneh Abbasi-Sureshjani, Alvaro Gomariz
F. Hoffmann-La Roche AG, Basel, Switzerland

Abstract

Digital pathology has significantly advanced disease detection and pathologist efficiency through the analysis of gigapixel whole-slide images (WSI). In this process, WSIs are first divided into patches, for which a feature extractor model is applied to obtain feature vectors, which are subsequently processed by an aggregation model to predict the respective WSI label. With the rapid evolution of representation learning, numerous new feature extractor models, often termed foundational models, have emerged. Traditional evaluation methods, however, rely on fixed aggregation model hyperparameters, a framework we identify as potentially biasing the results. Our study uncovers a co-dependence between feature extractor models and aggregation model hyperparameters, indicating that performance comparability can be skewed based on the chosen hyperparameters. By accounting for this co-dependency, we find that the performance of many current feature extractor models is notably similar. We support this insight by evaluating seven feature extractor models across three different datasets with 162 different aggregation model configurations. This comprehensive approach provides a more nuanced understanding of the relationship between feature extractors and aggregation models, leading to a fairer and more accurate assessment of feature extractor models in digital pathology.

1. Introduction

The field of digital pathology (DP) has rapidly evolved, offering automated solutions for critical tasks in pathology practise, such as breast cancer [8] or metastases detection [19]. Central to this innovation is the analysis of gigapixel whole-slide images (WSI) stained with H&E. The large size of these images poses a significant computational challenge, making the direct application of standard deep learning models for classification impractical. As a solution, the digital pathology community has widely adopted an adaptation of the multiple instance learning (MIL) framework.

With this MIL approach, as depicted in step 1 in Fig-

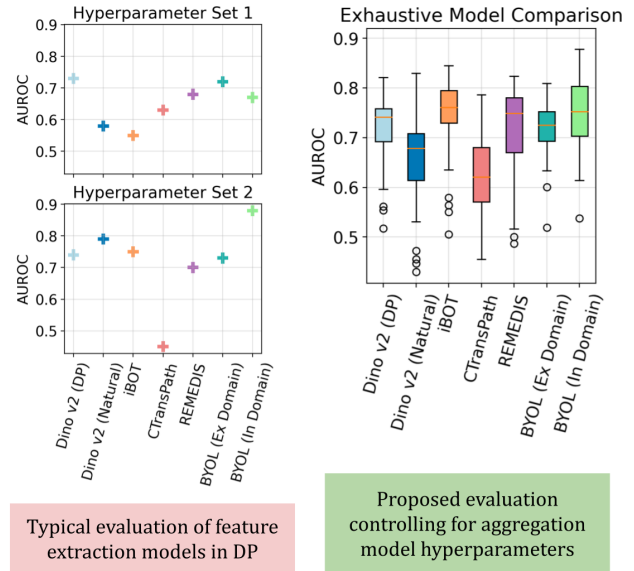


Figure 1. (left) Typical frameworks for evaluation of feature extraction models use fixed hyperparameters in the aggregation models, leading to substantially different results and hence limited informative value. (right) Our framework, which uses an extensive search over 81 aggregation model hyperparameters, shows a large range of results across these configurations, hence providing deeper insights into the actual performance of feature extraction models in digital pathology.

ure 2, the WSI is partitioned into smaller, more manageable patches, known as tiles. Features from these tiles are extracted using a *feature extractor* model, generating an embedding vector for each tile. Within the MIL framework, all embeddings corresponding to a single WSI, collectively referred to as *bag*, are assigned a common label. As shown in step 2 in Figure 2, an *aggregation model* or MIL model is applied to the bag to learn and predict its label [11, 21].

The employment of a feature extractor transcends mere computational efficiency. It is pivotal in addressing the limitations posed by scarce labeled data, a common challenge in DP. An optimal feature extractor, typically a pre-trained model, generates informative features across diverse datasets. These features can be effectively utilized by a

feature aggregation model, enabling efficient learning even with limited labeled data. This growing recognition of the importance of feature quality has spurred rapid progress into advanced representation learning techniques, aiming to develop more robust and informative features for digital pathology applications.

Since the pivotal work of Chen et al. [6], which significantly improved visual representations using contrastive learning (SimCLR), a range of novel representation learning approaches has been introduced. SimCLR learns representations by ensuring that the embeddings of images with the same label (positive examples) are close, whereas the embeddings of images with different labels (negative examples) are far apart. Subsequently, Grill et al. [14] showed that self-supervised learning can also be done without negative examples (BYOL) and this approach was further improved and combined with transformers leading to DINO [4]. The most recent approaches combine masked autoencoder (MAE) [15] with self-distillation. This is the strategy used by iBOT [28] and is also at the core of DINOv2 [22]. The improved representations lead to impressive unsupervised learning performance on a range of natural images tasks, closing the gap to supervised learning.

The adaptation of the advances in representation learning to learn better feature extractor for digital pathology has been significant. Two approaches which use contrastive learning for training the feature extractor for digital pathology are CTransPath [26] and REMEDIS [1]. Due to the large number of tiles that can be extracted from a single WSI and the availability of large publicly available datasets, such as TCGA [24], the datasets for CTransPath and REMEDIS contain 16 Mio and 50 Mio tiles, respectively. As representation learning tends to improve with a larger dataset and models, recent research efforts focus on increasing the dataset and model size while using more recent self-supervised learning methodologies. The aim of this effort is to obtain so called *foundational models* that are both generalizable and high performing. This would mitigate the requirement of re-training for every dataset. Filiot et al. [10] made a first step in this direction and demonstrated better classification performance compared to CTransPath by extracting feature embeddings using a model trained with iBOT. Chen et al. [5] went a step further and increased the dataset size to 100 Mio tiles while using DINOv2 to train the feature extraction model. Finally, the most recent feature extractor, Virchow [25], was also trained using the DINOv2 approach but on a dataset size of 380 Mio tiles.

Due to the rapidly increasing number of publications for feature extractor models and their rapid adoption in the field, it is now crucial to correctly compare different models. As described earlier, the feature extraction is only the first step in the classification pipeline for WSIs. Thus,

when comparing feature extraction models, the second step, where the embedding vectors are processed with an aggregation model to make the final prediction, should also be accounted for. Popular model choices for this second step are AttentionMIL [16] and TransMIL [23]. Typically, when evaluating different feature extractors, an aggregation model such as AttentionMIL, is trained with a fixed set of hyperparameters for every feature extraction model. However, as illustrated in Figure 1, the ranking of the best feature extraction model drastically depends on the set of hyperparameters are used for the aggregation model training.

In this paper, we show that whereas the feature extractor does indeed have some influence on the classification performance, the hyperparameter choices for the aggregation model largely dominates the results. This insight is confirmed by observing the performance fluctuation of a single feature extractor, when the aggregation model is trained with a wide range of hyperparameter sets. Thus, when comparing feature extractors, the second step of the classification pipeline, namely the aggregation model, is an important variable to control for. Our contribution in this paper is twofold.

- We reveal the interdependence between feature extractor models and aggregation model hyperparameters, challenging traditional feature extractor evaluation methods in digital pathology.
- We propose a framework for stringent and fair evaluation for state-of-the-art feature extractors.

2. Related Works

2.1. Feature Extraction

For the feature extraction step, it is crucial that as much information as possible is extracted of each tile, as that information can be leveraged in the subsequent classification. To extract features from the tiles, many models have been proposed. The models differ based on which dataset they are trained on, how large the model is and what learning paradigm is used. Here, we review some of the most recent and wide spread feature extraction models used in digital pathology.

ImageNet Models: ImageNet [9] has been an important benchmark dataset and many state-of-the-art models are trained on the dataset. Furthermore, the labels available for each image allow supervised training. Due to the easily available models trained on ImageNet, many digital pathology papers use them as feature extractors [16, 20]. However, the models come with the limitation that ImageNet is a natural image dataset and thus there is a domain gap to digital pathology images.

BYOL Models: The BYOL self-supervised learning approach [14] does not require negative samples, as is the case in contrastive learning, and is therefore often referred to as

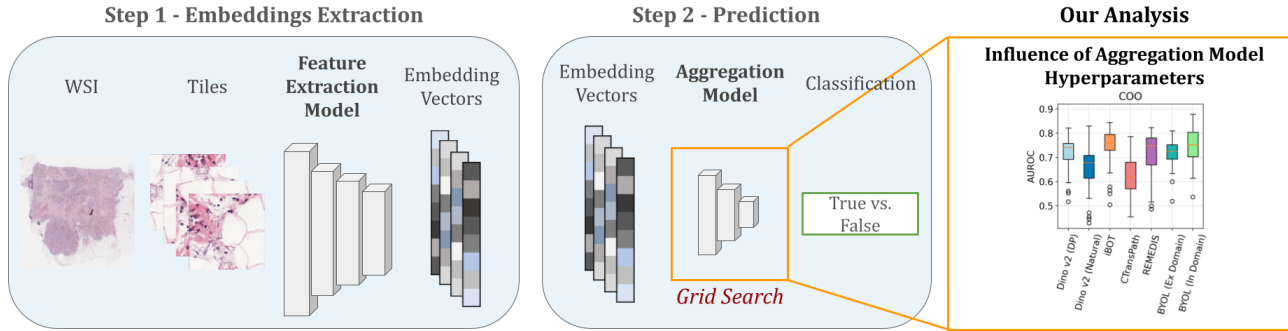


Figure 2. Illustration of the typical classification pipeline with MIL in digital pathology. As a first step, features are extracted from tiles of a WSI to create embedding vectors. In a second step, the embedding vectors are aggregated using an aggregation model which outputs a prediction for the WSI. Examples of classification tasks used in this study include HER2+ vs HER2-, ABC vs GCB, and cancer vs healthy patients. In our evaluation, we test different feature extraction models while focusing on an exhaustive grid search for the aggregation model hyperparameters to see if there is a co-dependence between the two models.

self-distillation [2]. This has as an important advantage for digital pathology, since labels are only assigned per WSI and are not specific to tiles. The absence of specific labels for the tiles makes BYOL one popular representation learning approach used when training feature extractors for digital pathology [12].

iBOT Models: Often, either a contrastive, self-distillation or masked autoencoder approach is used for self-supervised learning. With iBOT [28] the authors combined the masked autoencoder and self-distillation approach to benefit from each others abilities, showing strong feature extraction performance on natural images. An iBOT framework has been recently used to train a feature extractor for digital pathology [10].

DINOv2 Models: Recently, the new self-supervised learning approach DINOv2 [22] has been introduced which improves iBOT [28] by optimizing various losses and training parameters. In addition, the authors provided models which were trained on 142 Mio natural images and set a new state-of-the-art for feature extraction benchmarks. Due to the success of DINOv2, several researchers have recently used the DINOv2 framework to train models on digital pathology datasets [5, 25].

CTransPath [26]: This model is trained with contrastive learning and uses a modified MoCov3 approach [7]. Often in contrastive learning for digital pathology, every tile is considered unique and all other tiles are negative examples. The authors however propose to classify similar tiles in a batch as positive examples. The authors report better classification performance using their trained feature extractor compared to using other self-supervised learning frameworks.

REMEDIS [1]: This study takes advantage of the availability of large models trained on big natural image datasets. Furthermore, these models are specifically trained for trans-

fer learning [18]. To adapt these feature extracting models to digital pathology, the authors use the SimCLR.

2.2. Aggregation Methods

Aggregation methods have a rich literature and are continuously improving. In the context of the paper, we review two of the most widely spread approaches, namely AttentionMIL [16] and TransMIL [23]. When splitting a WSI into tiles for prediction, some assumptions need to be made about how to aggregate the predictions back to a single value that represents the whole WSI. A naive approach would be to say if any tile shows a positive label, for example indicating cancer, then the WSI should have a positive label. However, minor errors of such tile classification can easily have negative consequences. Both AttentionMIL and TransMIL use more sophisticated aggregation methods by utilizing attention with different underlying assumptions.

AttentionMIL: This method works under the assumption that, when aggregating information from the tiles, the order of the tiles does not matter and that there is no interdependency between the tiles. Nevertheless, some features from certain tiles might have a higher importance than the features of other tiles. For example, if one tile shows features related to cancer, the information of this tile should be weighted higher than when a tile shows no particular features. To this end, the authors introduce attention, which is the weight that is assigned to the features of each embedding when aggregating the features to make the final prediction for the WSI. Due to the simplicity of the approach as well as underlying assumption, this aggregation method has seen widespread adoption.

TransMIL: This method attempts to loosen the identical and independent assumption of the tile information and allow inter tile dependency. For example, some features of a tile may only become important if observed together with

features from another tile. This information would be disregarded by AttentionMIL. Allowing inter tile dependency can elegantly be achieved with the self-attention mechanism of transformers. For this work, the authors use the Nyströmformer [27] architecture and show favourable results compared to several aggregation methods.

3. Experimental Setup and Methods

We herein describe the pipeline employed for classification of WSI and present our hypotheses that challenge the evaluation frameworks typical in the literature. We also describe our experimental methodology to address those hypothesis, enabling a more thorough evaluation.

3.1. Pipeline for classification of WSIs

As shown in Figure 2, the typical MIL pipeline for digital pathology WSIs requires two models to obtain a final classification for a given WSI. In the first step, a feature extraction model is used. Due to the recent progress in self-supervised learning and large publicly available digital pathology datasets, these feature extraction models generalize well and are a first step towards foundational models in digital pathology [3, 5, 25]. The implication of this development means that the same feature extraction model can be used for wide range of tasks as well as different datasets. In the second step of the MIL pipeline, a smaller aggregation model is trained that takes the embedding vectors that were extracted for each tile of the WSI in the first step, and aggregates the information to make a final prediction. In contrast to the feature extraction model, this smaller aggregation model is re-trained for each dataset.

Previous studies mostly rely on frozen hyperparameters of the aggregation model when comparing feature extraction models [1, 5, 17]. This experimental setup assumes that the feature extraction model does not influence the optimal choice of aggregation model hyperparameters. Figure 1 clearly shows this assumption to be incorrect. Thus, this widely adopted evaluation framework for feature extraction models is suboptimal. Indeed, fixed aggregation model hyperparameters can favour some feature extraction models while penalizing others. We outline an experimental setup to thoroughly answer two related questions:

Question 1: Does an optimal aggregation model hyperparameter set exist, which is optimal for several feature extraction models?

Question 2: When controlling for aggregation model hyperparameters, how does the current state-of-the-art feature extraction models compare?

3.2. Feature Extraction Models

To answer these questions, we use seven different feature extraction models in our experiments. An overview of the models and their characteristics can be found in Table 1.

Firstly, we examine the potential of large models trained on natural images for the task of digital pathology feature extraction by investigating the state-of-the-art ViT-L model provided by the DINOv2 authors [22]. The model is trained on 142 Mio natural images and has 300 Mio parameters. We also investigate the performance of recently published models which are specifically trained on digital pathology datasets: CTransPath [26], REMEDIS [1] and iBOT [10]. The student model was used for iBOT as this was the default in the official codebase at the time of submission. All of these models are trained on large digital pathology datasets, as detailed in Table 1. Lastly, we investigate three feature extracting models trained in-house.

Recent feature extraction models trained with the DINOv2 self-supervised learning approach for digital pathology are not available yet [5, 25]. We include this state-of-the-art approach for our comparison by training a ViT-L feature extraction model from scratch. The model is trained on TCGA and a large in-house dataset with diverse tissue types and real-world data. The total training dataset size is 35 Mio 224×244 tiles. WSIs are usually acquired at different magnifications. Tiles from $20\times$ (lower) magnification WSIs have more content than those from $40\times$ (higher) magnification. However, $40\times$ tiles capture more details of the depicted tissue due to their higher resolution. We train on both $20\times$ and $40\times$ magnification, a strategy that has been shown to be beneficial [17]. We employ the official DINOv2 repository with the default parameters for ViT-L/16 training, with a few exceptions. We decrease the batch size to 352 due to computational constraints. Due to the decreased batch size, we increase the number of epochs to 270, warm-up epochs to 25 and adjust the learning rate to 1.375×10^{-3} according to the heuristic by Goyal et al. [13].

We also train two ResNet-50 feature extractors with the BYOL self-supervised learning approach. We train one model on 2 Mio tiles, $20\times$ magnification, which are randomly sampled from the TCGA dataset. The aim of this model is to be a lower bound of models trained on digital pathology images. The reason being that both the model size and training dataset size are smaller than other models we compare against. We refer to this model as $\text{BYOL}_{\text{ExDomain}}$ since the training dataset does not overlap with the evaluation dataset and we use it to evaluate the performance gap to larger, foundational, feature extraction models. For the second ResNet-50 model trained with BYOL, we again use a 2 Mio tile dataset. In this model, the tiles are randomly sampled from the datasets on which the models are evaluated on. Thus even though the training dataset is small compared to the other published models, there is no domain gap between the dataset on which it is trained and evaluated on. For this reason, we label the model as $\text{BYOL}_{\text{InDomain}}$. Due to the lack of a domain gap the model should also represent a higher bound for perfor-

	Learning Approach	Model Details	Model Size (Mio.)	Embed. Size	Dataset Content	Dataset Size / Tiles (Mio.)	In-house training
Dino v2 (DP)	Combination	ViT-L/16	300	1024	TCGA + in-house	35	yes
Dino v2 (Natural)	Combination	ViT-L/14 distilled	300	1024	LVD-142M (natural images)	142	no
iBOT	Combination	ViT-B	86	768	TCGA	43	no
CTransPath	Contrastive Learning	Swin Transformer	280	768	TCGA + PAIP	16	no
REMEDIS	Contrastive Learning	BiT-M (ResNet-152x2)	240	4096	TCGA	50	no
BYOL (Ex Domain)	Self-distillation	ResNet50	26	2048	TCGA	2	yes
BYOL (In Domain)	Self-distillation	ResNet50	26	2048	DLBCL, Herohe, Camelyon16	2	yes

Table 1. List of the feature extraction models used for evaluation with some of their key properties.

mance.

3.3. Aggregation Model Hyperparameters

To investigate the performance fluctuation of the MIL pipeline when the feature extraction model is fixed and the aggregation model hyperparameters change, we use two aggregation models, namely AttentionMIL [16] and TransMIL [23].

For each architecture, we evaluate four different hyperparameters with three values each as shown in Table 2. These are decided heuristically with preliminary experiments assessing the influence and effective range of each hyperparameter. The resulting 81 different hyperparameter configurations are outlined below for each aggregation model.

Hyperpar.	AttentionMIL	TransMIL
Learn. rate	1e-4, 1e-3, 1e-2	1e-5, 1e-4, 1e-3
Bag size	128, 1024, 8192	128, 1024, 2048
Layers	(512), (512, 384, 384), (512, 256, 128, 64, 32)	1, 2, 3
Dropout	0.00, 0.25, 0.50	0.00, 0.25, 0.50

Table 2. Set of hyperparameter values for each aggregation model. Layers refer to fully connected layers in AttentionMIL and to attention blocks in TransMIL.

AttentionMIL: When creating a batch for the aggregation model during training, there are two relevant parameters. One is the *bag size*, which determines the amount of tiles that is sampled from a particular WSI. The second is the *bags per batch*, determining how many bags from different WSIs are collected to form a batch. Here, we vary only the bag size parameter since it showed a larger influence. The Layers (fully connected layers) parameter corresponds to the architecture choice of the aggregation model. The list of numbers indicate the number of nodes for each layer.

Lastly, the dropout parameter refers to the dropout which is applied at every layer of the aggregation model.

TransMIL: The selected hyperparameters for TransMIL are different due to the model architecture being a transformer and not consisting of fully connected layers. Instead of changing the number of FC layers and their respective number of nodes, for TransMIL we vary the number of Nyströmformer attention blocks. Furthermore, we also reduce the maximal bag size to 2048 due to computational limitations.

The rest of the parameters for both AttentionMIL and TransMIL training are fixed. We use a weight decay of 10^{-5} , bags per batch of 4, AdamW optimizer, weighted cross entropy loss, and cosine annealing scheduler. We train all of the aggregation models for 50 epochs, which always converge for our hyperparameter ranges.

3.4. Evaluation Datasets

We assess the performance of feature extraction models in binary classification across three distinct digital pathology datasets. This approach guarantees that our findings are robust and not confined to a single dataset, thereby providing a more generalizable answer to our research questions. These datasets consist of WSIs of H&E-stained histopathology slides. On each dataset we evaluate the performance of every feature extractor using all the possible hyperparameter sets for the aggregation model being used. This setup results in 81 different hyperparameter sets for 7 feature extraction models, 2 aggregation models and 3 datasets, leading to a comparison of $81 \times 7 \times 2 \times 3 = 3402$ experiments.

In evaluating the binary classification performance of each configuration, we utilized the area under the receiver operating characteristic curve (AUROC) as well as average precision (AP). Both AUROC and AP range from 0 to 1. A higher AUROC score indicates that the model has a better capability to distinguish between the positive and negative classes, thus correctly identifying true positives and

true negatives. A higher AP score shows that the model more accurately predicts positive instances across all levels of recall, effectively balancing precision and recall. The metric for every evaluation on the test set is obtained by using the aggregation model parameters at the epoch with highest validation score during training.

COO: Binary classification of cell of origin (COO). Each image contains the COO prediction label of activated B-cell like (ABC) or germinal center B-cell like (GCB) tumors in diffuse large B-cell lymphoma (DLBCL). 709 WSIs from two internal datasets were used. This data closely mirrors real-world data, since it is crucial to assess classification approaches in digital pathology using such data and tasks. The WSIs (40× magnification) have been scanned by Ventana DP200 scanners. The artifact-free tissue tiles of this dataset were combined and randomly split into 70% training set, 15% validation set and 15% test set.

Camelyon16: Binary classification of cancer metastases vs. healthy in H&E images of lymph node tissue. The Camelyon16 dataset [19] consists of 400 WSIs of sentinel lymph nodes. The dataset is publicly available. For our evaluation, all artifact-free tissue tiles were used as well as the official train-test split. 20% of the training data was used as the validation set.

Herohe: Binary classification of breast cancer human epidermal growth factor receptor 2 (HER2) using the publicly available Herohe [8] dataset. Each H&E stained WSI is either labeled as HER2 positive or HER2 negative. We use the artifact-free tiles from tumor regions detected with an in-house tumor segmentation model. The 508 WSIs are split according to the official train-test split. 20% of the training data is used as the validation set.

4. Results

In this section, we answer the questions posed in Section 3. First, we examine if an optimal aggregation model hyperparameter set exists, which is optimal for several feature extraction models. Subsequently, we compare the performance of different feature extraction models while considering the fluctuation of performance observed for different aggregation model hyperparameters.

4.1. Aggregation Model Influence

Hyperparameters play a crucial role in machine learning. Thus, it is expected to encounter classification performance fluctuations when changing the aggregation model hyperparameters. We herein examine how large the performance fluctuation is and if there is a co-dependency between the feature extraction models and aggregation model hyperparameters. The latter is already qualitatively confirmed by the motivating Figure 1, where we observe that the ranking for the best feature extractor model changes based on the chosen aggregation model hyperparameter set.

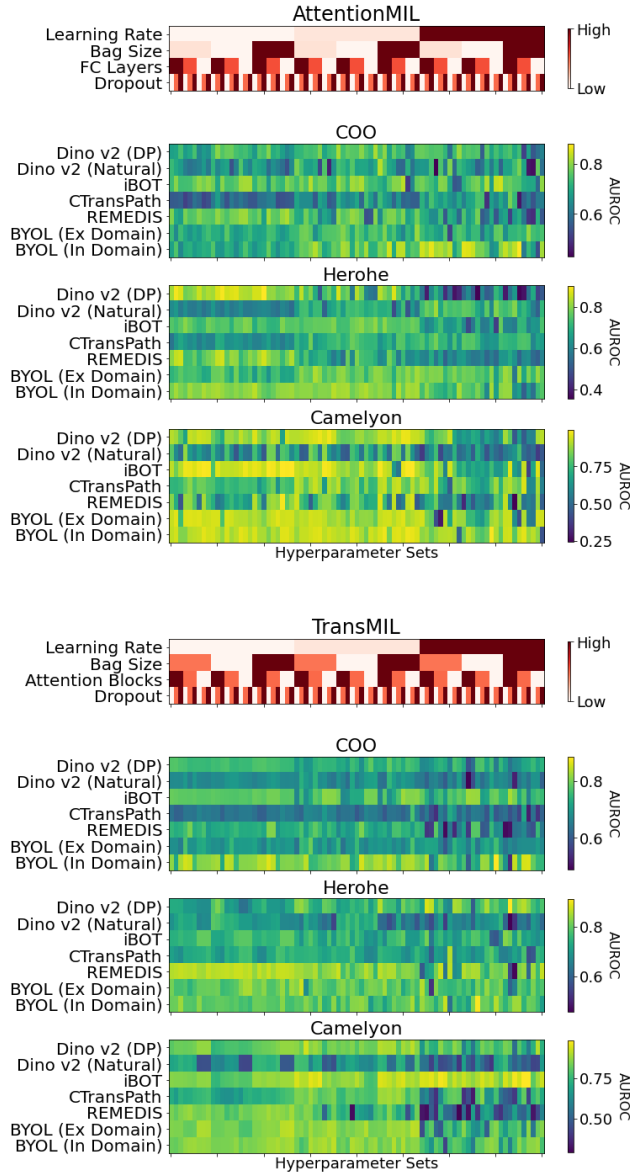


Figure 3. The heatmap shows the performance of every aggregation model hyperparameter set for each feature extraction model. The lighter the colour the higher the AUROC. The heatmaps are shown for all three datasets and for both AttentionMIL and TransMIL approaches. The red colored legend shows how the hyperparameter sets are ordered on the heatmap. For example, the lowest learning rate is used for the first third of the hyperparameter sets, followed by the next higher learning rate. The legend should facilitate detecting hyperparameters sets with consistently high performance. However, no clear patterns are visible in the heatmaps indicating that aggregation model hyperparameters need to be accounted for when comparing feature extraction models.

Figure 3 offers more insight into the effect of different hyperparameters by showing the classification performance for every hyperparameter set and feature extraction model

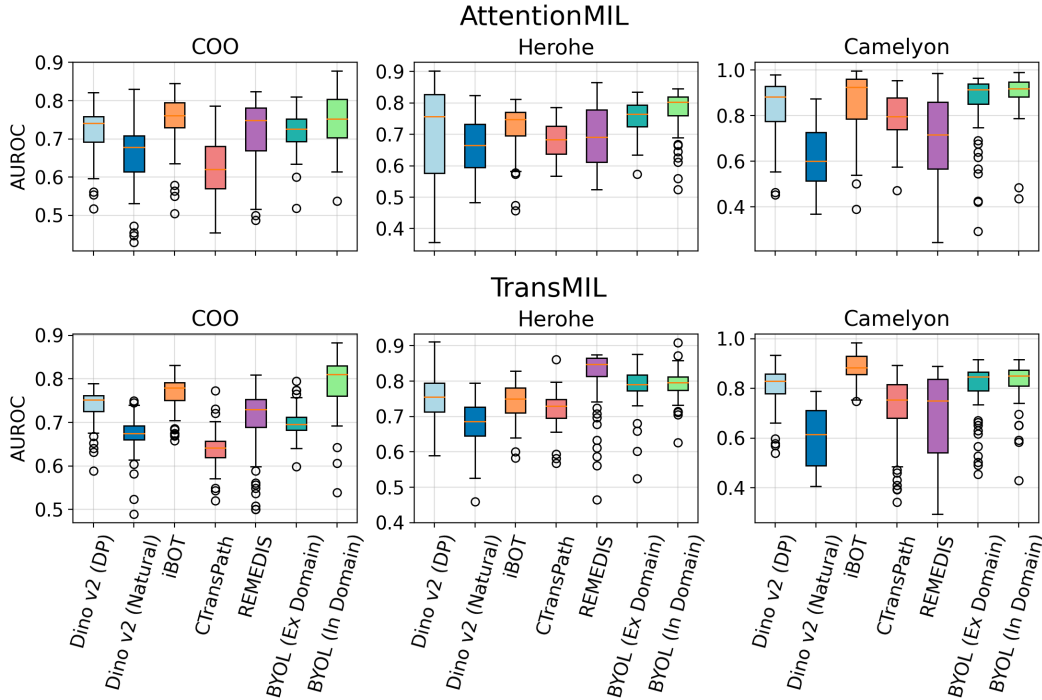


Figure 4. Here, we compare seven feature extraction models while accounting for different aggregation model hyperparameter sets. Specifically, each boxplot represents the performance range when fixing the feature extraction model by using 81 different hyperparameter sets for the aggregation model. We show this for three different datasets and for both AttentionMIL and TransMIL approaches. From the boxplots it can be seen that the performance fluctuation is large as well as the overlap between different feature extraction models.

as a heatmap. This heatmap, showing the AUROC score, shows similar trends as the one with the AP score shown in the supplementary. The legend above the heatmaps is included to facilitate detecting patterns in the heatmaps. For example the hyperparameter sets with the lowest learning rate are to the left of the heatmap, which are seen to produce worse performance in the case of the COO dataset with CTransPath. From this figure we can conclude two things.

No optimal hyperparameter: There does not seem to be a set of hyperparameters for the aggregation model that leads to superior results across feature extraction models. This would be clearly visible with a bright column spanning across all the feature extractor models.

Dataset-specific hyperparameters: Even when examining the best aggregation model hyperparameter set for a single feature extraction model no clear trend is visible. For some datasets and feature extraction models, the optimal learning rate seems to be important when using AttentionMIL. For TransMIL the number of attention blocks are more relevant. This can be seen by the patterns of the legend being replicated in the heatmaps. However, for most datasets and feature extraction models, no clear pattern from the color-coded hyperparameters are replicated in the heatmaps. This indicates that even for a single feature extractor model the

best performing MIL hyperparameter set is not obvious and requires investigation.

Given the limitation of finding an optimal hyperparameter set, a distribution of hyperparameters should be considered when comparing feature extraction models. Otherwise, the improved performance of one feature extraction model over another could solely be due to the chosen aggregation model hyperparameter set.

4.2. Feature Extractor Comparison

As seen above, when developing new feature extractor models, it is crucial to carefully evaluate the performance gain compared to previous models. In Figure 4, we visualize the performance of feature extractor models across different datasets. Instead of showing a single result for a fixed aggregation model hyperparameter set, which is common practice in literature, we show the results of the feature extractor model over all 81 hyperparameter sets. We use box plots to effectively visualize the corresponding metrics. The performance variation linked to different aggregation model hyperparameters, previously observed in Figure 3, is reflected here in the vertical spread of the box plots. The large range of the boxes indicate that the overlap of the performance between different feature extractors is large. Re-

markably, there are some clear trends to be noted despite these large ranges of results.

Training on DP datasets is necessary: The DINOv2 model trained on natural images performs poorly compared to all other models, consistently for all the datasets. From this we can conclude that it is indeed important to train feature extraction models on digital pathology datasets.

Small and large models perform similar: The relatively small model $BYOL_{ExDomain}$ performs similarly to larger models, which are trained on larger datasets, such as $DINOv2_{DP}$ and iBOT. This implies that larger models are not necessarily better for digital pathology. A similar observation was made by Filiot et al. [10] where a ViT-B model performed better than a ViT-L model.

Feature extractors generalize well: The feature extractor that is trained on the WSIs of the evaluation dataset ($BYOL_{InDomain}$) performs well on all the datasets as expected. However, the median performance of $BYOL_{InDomain}$ is not much higher than that of other models such as $DINOv2_{DP}$, iBOT and $BYOL_{ExDomain}$. This indicates that the feature extraction models have the capability to generalize well.

5. Conclusion

In this study, we challenge the prevailing methodology for comparing feature extractor models in digital pathology literature, demonstrating that it may yield misleading results. Our investigation highlights that relying solely on a single aggregation model hyperparameter set can disproportionately favor certain feature extractor models while disadvantaging others. Our comprehensive analysis, taking into account performance variations across multiple hyperparameter sets of the aggregation model, reveals a considerable overlap in performance between different feature extractor models. Significantly, we find no universal aggregation model hyperparameter set that is uniformly effective for all feature extractors. Our work is limited though by only looking at classification tasks. In addition, the DINOv2 model we trained on digital pathology images might be subpar to other models due to computational and dataset limitations. Nevertheless, we believe this work will contribute to a more nuanced evaluation of feature extractor models that will help gain insight and further accelerate this rapidly evolving field.

References

- [1] Shekoofeh Azizi, Laura Culp, Jan Freyberg, Basil Mustafa, Sebastien Baur, Simon Kornblith, Ting Chen, Nenad Tomasev, Jovana Mitrović, Patricia Strachan, et al. Robust and data-efficient generalization of self-supervised machine learning for diagnostic imaging. *Nature Biomedical Engineering*, pages 1–24, 2023. 2, 3, 4
- [2] Randall Balestriero, Mark Ibrahim, Vlad Sobal, Ari Morcos, Shashank Shekhar, Tom Goldstein, Florian Bordes, Adrien Bardes, Gregoire Mialon, Yuandong Tian, et al. A cookbook of self-supervised learning. *arXiv preprint arXiv:2304.12210*, 2023. 3
- [3] Rishi Bommasani, Drew A Hudson, Ehsan Adeli, Russ Altman, Simran Arora, Sydney von Arx, Michael S Bernstein, Jeannette Bohg, Antoine Bosselut, Emma Brunskill, et al. On the opportunities and risks of foundation models. *arXiv preprint arXiv:2108.07258*, 2021. 4
- [4] Mathilde Caron, Hugo Touvron, Ishan Misra, Hervé Jégou, Julien Mairal, Piotr Bojanowski, and Armand Joulin. Emerging properties in self-supervised vision transformers. In *Proceedings of the IEEE/CVF international conference on computer vision*, pages 9650–9660, 2021. 2
- [5] Richard J Chen, Tong Ding, Ming Y Lu, Drew FK Williamson, Guillaume Jaume, Bowen Chen, Andrew Zhang, Daniel Shao, Andrew H Song, Muhammad Shaban, et al. A general-purpose self-supervised model for computational pathology. *arXiv preprint arXiv:2308.15474*, 2023. 2, 3, 4
- [6] Ting Chen, Simon Kornblith, Mohammad Norouzi, and Geoffrey Hinton. A simple framework for contrastive learning of visual representations. In *International conference on machine learning*, pages 1597–1607. PMLR, 2020. 2
- [7] Xinlei Chen*, Saining Xie*, and Kaiming He. An empirical study of training self-supervised vision transformers. *arXiv preprint arXiv:2104.02057*, 2021. 3
- [8] Eduardo Conde-Sousa, João Vale, Ming Feng, Kele Xu, Yin Wang, Vincenzo Della Mea, David La Barbera, Ehsan Montahaei, Mahdieh Baghshah, Andreas Turzynski, Jacob Gildenblat, Eldad Klaiman, Yiyu Hong, Guilherme Aresta, Teresa Araújo, Paulo Aguiar, Catarina Eloy, and Antonio Polónia. Herohe challenge: Predicting her2 status in breast cancer from hematoxylin&eosin whole-slide imaging. *Journal of Imaging*, 8(8), 2022. 1, 6
- [9] Jia Deng, Wei Dong, Richard Socher, Li-Jia Li, Kai Li, and Li Fei-Fei. Imagenet: A large-scale hierarchical image database. In *2009 IEEE conference on computer vision and pattern recognition*, pages 248–255. Ieee, 2009. 2
- [10] Alexandre Filiot, Ridouane Ghermi, Antoine Olivier, Paul Jacob, Lucas Fidon, Alice Mac Kain, Charlie Saillard, and Jean-Baptiste Schiratti. Scaling self-supervised learning for histopathology with masked image modeling. *medRxiv*, pages 2023–07, 2023. 2, 3, 4, 8
- [11] Michael Gadermayr and Maximilian Tschuchnig. Multiple instance learning for digital pathology: A review on the state-of-the-art, limitations & future potential. *arXiv preprint arXiv:2206.04425*, 2022. 1

- [12] Jacob Gildenblat, Anil Yüce, Samaneh Abbasi-Sureshjani, and Konstanty Korski. Deep cellular embeddings: An explainable plug and play improvement for feature representation in histopathology. In *International Conference on Medical Image Computing and Computer-Assisted Intervention*, pages 776–785. Springer, 2023. [3](#)
- [13] Priya Goyal, Piotr Dollár, Ross Girshick, Pieter Noordhuis, Lukasz Wesolowski, Aapo Kyrola, Andrew Tulloch, Yangqing Jia, and Kaiming He. Accurate, large mini-batch sgd: Training imagenet in 1 hour. *arXiv preprint arXiv:1706.02677*, 2017. [4](#)
- [14] Jean-Bastien Grill, Florian Strub, Florent Althé, Corentin Tallec, Pierre Richemond, Elena Buchatskaya, Carl Doersch, Bernardo Avila Pires, Zhaohan Guo, Mohammad Gheshlaghi Azar, et al. Bootstrap your own latent—a new approach to self-supervised learning. *Advances in neural information processing systems*, 33:21271–21284, 2020. [2](#)
- [15] Kaiming He, Xinlei Chen, Saining Xie, Yanghao Li, Piotr Dollár, and Ross Girshick. Masked autoencoders are scalable vision learners. In *Proceedings of the IEEE/CVF conference on computer vision and pattern recognition*, pages 16000–16009, 2022. [2](#)
- [16] Maximilian Ilse, Jakub Tomczak, and Max Welling. Attention-based deep multiple instance learning. In *International conference on machine learning*, pages 2127–2136. PMLR, 2018. [2](#), [3](#), [5](#)
- [17] Mingu Kang, Heon Song, Seonwook Park, Donggeun Yoo, and Sérgio Pereira. Benchmarking self-supervised learning on diverse pathology datasets. In *Proceedings of the IEEE/CVF Conference on Computer Vision and Pattern Recognition*, pages 3344–3354, 2023. [4](#)
- [18] Alexander Kolesnikov, Lucas Beyer, Xiaohua Zhai, Joan Puigcerver, Jessica Yung, Sylvain Gelly, and Neil Houlsby. Big transfer (bit): General visual representation learning. In *Computer Vision—ECCV 2020: 16th European Conference, Glasgow, UK, August 23–28, 2020, Proceedings, Part V 16*, pages 491–507. Springer, 2020. [3](#)
- [19] Geert Litjens, Peter Bandi, Babak Ehteshami Bejnordi, Oscar Geessink, Maschenka Balkenhol, Peter Bult, Altuna Halilovic, Meyke Hermsen, Rob van de Loo, Rob Vogels, Quirine F Manson, Nikolas Stathonikos, Alexi Baidoshvili, Paul van Diest, Carla Wauters, Marcory van Dijk, and Jeroen van der Laak. 1399 H&E-stained sentinel lymph node sections of breast cancer patients: the CAMELYON dataset. *GigaScience*, 7(6):giy065, 2018. [1](#), [6](#)
- [20] Ming Y Lu, Drew FK Williamson, Tiffany Y Chen, Richard J Chen, Matteo Barbieri, and Faisal Mahmood. Data-efficient and weakly supervised computational pathology on whole-slide images. *Nature biomedical engineering*, 5(6):555–570, 2021. [2](#)
- [21] Oded Maron and Tomás Lozano-Pérez. A framework for multiple-instance learning. *Advances in neural information processing systems*, 10, 1997. [1](#)
- [22] Maxime Oquab, Timothée Darcet, Théo Moutakanni, Huy Vo, Marc Szafraniec, Vasil Khalidov, Pierre Fernandez, Daniel Haziza, Francisco Massa, Alaaeldin El-Nouby, et al. Dinov2: Learning robust visual features without supervision. *arXiv preprint arXiv:2304.07193*, 2023. [2](#), [3](#), [4](#)
- [23] Zhuchen Shao, Hao Bian, Yang Chen, Yifeng Wang, Jian Zhang, Xiangyang Ji, et al. Transmil: Transformer based correlated multiple instance learning for whole slide image classification. *Advances in neural information processing systems*, 34:2136–2147, 2021. [2](#), [3](#), [5](#)
- [24] Katarzyna Tomczak, Patrycja Czerwińska, and Maciej Wiznerowicz. Review the cancer genome atlas (tcga): an immeasurable source of knowledge. *Contemporary Oncology/Współczesna Onkologia*, 2015(1):68–77, 2015. [2](#)
- [25] Eugene Vorontsov, Alican Bozkurt, Adam Casson, George Shaikovski, Michal Zelechowski, Siqi Liu, Philippe Mathieu, Alexander van Eck, Donghun Lee, Julian Viret, et al. Virchow: A million-slide digital pathology foundation model. *arXiv preprint arXiv:2309.07778*, 2023. [2](#), [3](#), [4](#)
- [26] Xiyue Wang, Sen Yang, Jun Zhang, Minghui Wang, Jing Zhang, Wei Yang, Junzhou Huang, and Xiao Han. Transformer-based unsupervised contrastive learning for histopathological image classification. *Medical image analysis*, 81:102559, 2022. [2](#), [3](#), [4](#)
- [27] Yunyang Xiong, Zhanpeng Zeng, Rudrasis Chakraborty, Mingxing Tan, Glenn Fung, Yin Li, and Vikas Singh. Nystromformer: A nystrom-based algorithm for approximating self-attention. In *Proceedings of the AAAI Conference on Artificial Intelligence*, pages 14138–14148, 2021. [4](#)
- [28] Jinghao Zhou, Chen Wei, Huiyu Wang, Wei Shen, Cihang Xie, Alan Yuille, and Tao Kong. ibot: Image bert pre-training with online tokenizer. *arXiv preprint arXiv:2111.07832*, 2021. [2](#), [3](#)

Aggregation Model Hyperparameters Matter in Digital Pathology

Supplementary Material

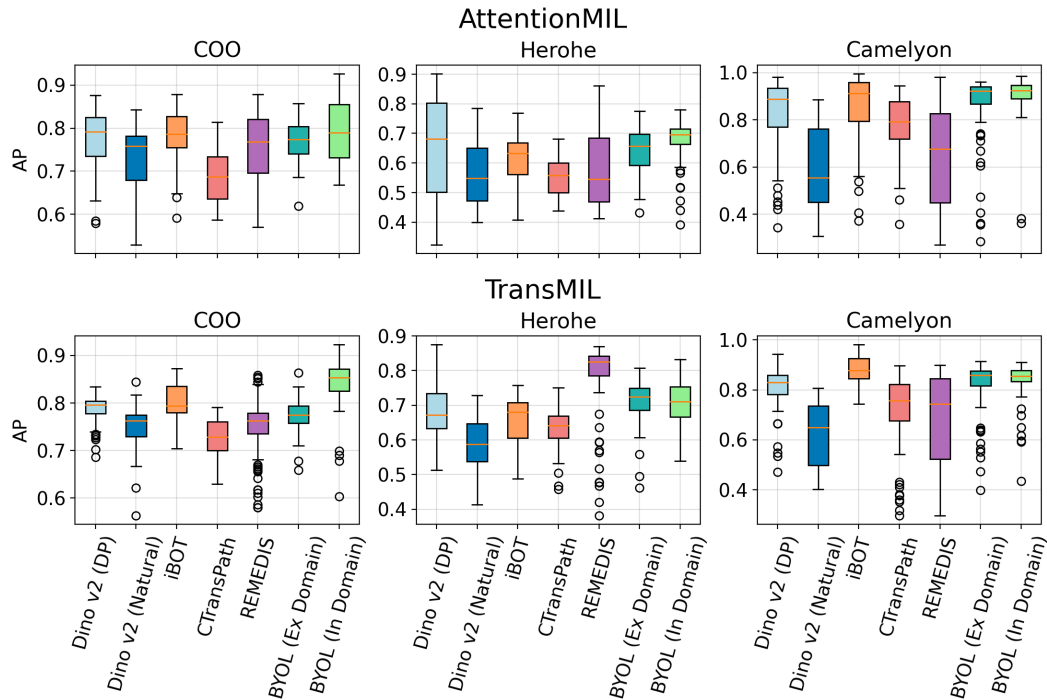


Figure 5. Here, we use the average precision (AP) metric to compare seven feature extraction models while accounting for different aggregation model hyperparameter sets. Specifically, each boxplot represents the performance range when fixing the feature extraction model by using 81 different hyperparameter sets for the aggregation model. We show this for three different datasets and for both AttentionMIL and TransMIL approaches. From the boxplots it can be seen that the performance fluctuation is large as well as the overlap between different feature extraction models. Furthermore, the boxplots show a similar trend when compared to using AUROC as metric.

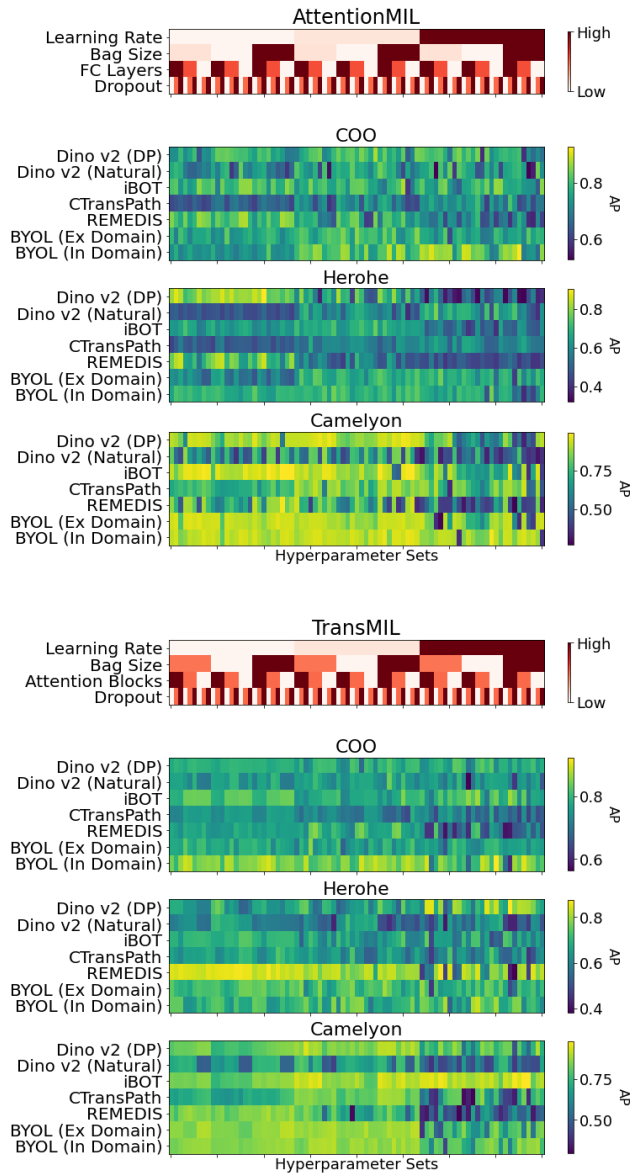


Figure 6. The heatmap shows the performance of every aggregation model hyperparameter set for each feature extraction model according to the AP metric. The lighter the colour the higher the AP. The heatmaps are shown for all three datasets and for both AttentionMIL and TransMIL approaches. The red colored legend shows how the hyperparameter sets are ordered on the heatmap. For example, the lowest learning rate is used for the first third of the hyperparameter sets, followed by the next higher learning rate. The legend should facilitate detecting hyperparameters sets with consistently high performance. However, no clear patterns are visible in the heatmaps indicating that aggregation model hyperparameters need to be accounted for when comparing feature extraction models. We observe similar trends compared to when using AUROC as a metric.